Osteopontin in colitis-associated carcinoma

Running title: Osteopontin in colitis-associated carcinoma

Subhakankha Manna[1§], Maximilian Sehn[2§], Danielle Cardoso da Silva[1§], Jakob J. Wiese[1], Claudia Heldt[1], Izabela Plumbom[3], Thomas Conrad[3], Cora C. Husemann[4], Karsten Kleo[4]., Lorena Derêzanin[6], Violaine Dony[1], Saeed K. Farahani[5], Franziska Weiss[5], Federica Branchi[1], Anja A. Kühl[1], Simon Schallenberg[4], January Weiner[6], Sefer Elezkurtaj[4], Benjamin Weixler[2], Jörn Gröne[2], Britta Siegmund[1], Michael Hummel[4], Michael Schumann[1$].

[1]Charité Universitätsmedizin Berlin, Department for Gastroenterology, Rheumatology and Infectious Diseases, Berlin, Germany.

[2]Charité Universitätsmedizin Berlin, Department of Visceral Surgery, Berlin, Germany.

[3]Max-Delbrueck-Center for Molecular Medicine, BIH/MDC Genomics Platform, Berlin, Germany.

[4]Charité Universitätsmedizin Berlin, Institute of Pathology and Molecular Pathology, Berlin, Germany.

[5]Charité Universitätsmedizin Berlin, Institute for Clinical Physiology, Berlin, Germany

[6]Bioinformatics, Berlin Institute of Health, BIH

Charite Universitatsmedizin Berlin,

[§], equally contributing

[$], corresponding author: michael.schumann@charite.de

Abstract

Patients with ulcerative colitis (UC) and Crohn's disease (CD) face a lifelong risk of developing colitis-associated carcinoma (CAC). Current insights into CAC development originate from murine CAC models, while human CAC studies primarily focus on mutational analysis of patient samples. Although the mutational landscape reveals distinct patterns and frequencies compared to colorectal cancer, it falls short in elucidating the inflammatory mechanisms of CAC development. Consequently, we adopted a multi-omics approach to unravel CAC carcinogenesis from an immunological perspective. Our data revealed a robust upregulation of *SPP1* gene in CAC at both RNA and protein levels, expressed by *CD68*+ macrophages. In vitro OPN stimulation demonstrated no direct effect on intestinal epithelial organoids. However, the mutually exclusive spatial location of *SPP1/OPN*+ macrophages and *CD8*+ T cells suggests a crucial indirect role of *SPP1/OPN* in mediating an immunosuppressive tumour microenvironment.

Introduction

About 0.4% of Europeans suffer from one of the two inflammatory bowel diseases, Crohn´s disease (CD) or ulcerative colitis (UC). Besides the significant reduction in quality of daily life in active CD or UC secondary to chronic diarrhea, hematochezia, episodes of severe abdominal pain and reduced physical fitness, these diseases pose an increased risk to patients to develop colitis-associated carcinoma (CAC) [1, 2]. In numbers, CAC accounts for approx. 10-15% of deaths in IBD patients [3]. In a study that exploited carcinoma findings in UC surveillance colonoscopies, the cumulative incidence of CAC was described to rise from 2.5% at 20 years to 7.6% at 30 years of colitis duration [4]. The advent of targeted therapies using biologicals has contributed to a reduction of CAC occurrence, pointing to the role of mucosal inflammation in colitis-associated carcinogenesis [3]. Nevertheless, a more recent meta-analysis identified the relative risk of patients suffering from inflammatory bowel disease to develop CAC to be 2.4-fold higher compared to the risk of the general population developing sporadic colorectal carcinoma (CRC) [5].

Differences in clinical presentation as rapid progression, presentation of CACs as interval carcinomas and occurrence of gene mutations distinct from sporadic CRC point to a CAC-specific tumor biology. As such, APC mutations, which are a cause for nuclear b-catenin translocation and consecutive stimulation of cell growth and inhibition of apoptosis, occur not as an initial step as found in sporadic CRCs but as a late carcinogenetic event [6, 7]. Moreover, mutations of the TP53 gene occur early on in CAC, prolong the activation of NF-kB signaling, aggravate the extent of colitis and accelerate the progression to high grade dysplasia and invasive carcinoma while TP53 is mutated only as a rather late step in sporadic CRCs [7, 8]. Another significant discrepancy to CRCs involves the role of pro-inflammatory cytokines as interleukin-6 (IL-6), IL-11, IL-22 and TNF-α [9-11]. Signaling of these cytokines occurs through kinase cascades including JAK/STAT, MAPK, PI-3 kinase and regulates expression of a multitude of putative tumor-relevant target genes including cytokine and cytokine receptor genes as IL-21, IL-21R and IL-23R and further transcription factors as RORγT, IRF4, and Batf [12]. Moreover, it was shown, that IL-22 and its natural counterpart IL-22 binding protein are directly involved in murine colon carcinogenesis [13]. One mechanism, by which cytokines as IL-22 or TGF-b may contribute to carcinoma development is

epithelial-to-mesenchymal transformation (EMT) [14, 15]. In this study, we identify another cytokine, osteopontin (OPN), to be highly expressed in inflammation-associated carcinogenesis in IBD patients.

Results

Clinical characteristics of the patients included in the study

To better understand CAC pathogenesis, patients who underwent surgery and were diagnosed with Crohn's disease-colitis, ulcerative colitis, colitis-associated colon cancer or sporadic colorectal cancer were retrospectively recruited from the Charité database after approval by the Charité ethical commission (EA/1/204/14). Inflammation-free borders of colon resections of diverticulitis patients were selected as the control population. CAC patients were categorized according to the previous IBD condition of the patients in Crohn's disease-associated CAC (CDAC) and ulcerative colitis-associated CAC (UCAC). In total, 20 CAC´s were included, that were in the majority of the mucinous type on histologic examination (**Table 1**). Of note, the inflammatory colitis activity in patients with IBD was higher when compared to the CAC patients, as the surgery in these patients was performed for their IBD, while the need for surgery in the CAC patients resulted from the carcinoma (**Table 1**).

Differential gene expression in colitis-associated carcinoma compared to colitis

To have a comprehensive view on differential gene expression in CAC, we compared the gene expression in colon tissues of patients with an IBD-associated colon carcinoma to either Crohn's colitis or UC surgical colon samples. For that, a Nanostring analysis was performed examining 654 genes (624 genes from the human immunology panel plus 30 custom genes). SPP1 gene was robustly upregulated in both UCCAC and CDCAC **(Figure 1B)**. Heatmaps of the 20 most upregulated and 20 most downregulated genes for CDAC vs. CD and UCAC vs. UC showed that CD and CDAC patients clustered separate from each other (**Figure 1C**) and that the clustering was almost perfect for UC and UCAC patients except for one UC patient (**Figure 1C**). The differentially regulated genes are listed in **Tables 2 and 3**. SPP1, the gene for osteopontin (OPN), was found to be the most upregulated gene in both comparisons, even though the two patient groups analyzed were totally independent from each other. Other significantly regulated genes included genes of cell signaling pathways (MAPK/ERK, DUSP4, SRC), chemokine genes and B-cell genes. Gene set analysis revealed genes for the adaptive immune system, lymphocyte activation and chemokine signaling to be mostly downregulated (**Table 4**).

Expression of OPN, its cellular source and disease prognosis

Since OPN was independently found as the most up-regulated gene in both comparisons, we decided to further investigate it. Analysis of the OPN counts from the Nanostring evaluation revealed a significant scatter, especially for the CAC conditions, with two separate groups of patients expressing either high or low OPN (**Figure 1C**). Stratifying patients along these groups (i.e., high or low OPN expressers) showed a tendency for a lower survival rate of the high OPN-expressing patients (**Figure 1D**), even though this correlation did not reach statistical significance. Analysis of OPN protein levels by a multi-staining immunehistological approach confirmed not only the strong upregulation in CAC samples but revealed furthermore a significant inhomogeneity when larger areas of tumor tissues were examined by stitching large tumor sections (in average approx. 5000 µm in diameter) after spinning disk imaging (**Figure 1E**). The majority of OPN-expressing cells were identified to be monocytes by CD68 immunostaining and – to a significant lesser extent – myenteric plexus cells (**Figure 1E**). Spatial

resolution of RNA expression (10x Genomics, Xenium platform) confirmed the strong SPP1 expression in CAC tissue and further subclassified OPN-expressing cells as *CD68+ macrophages* (**Figure 2A**)*,* and identified a macrophage subset in CAC that are *SPP1+ APOE+ CD163+* (**Figure 2C, Supplementary Fig 1**). SPP1 clusters were consistent across CAC patients but not in UC patients (**Supplementary Fig 1**). Moreover, the analysis of OPN expression by splice variant-specific probes allowed the identification of the prevailing OPN splice variant in CACs to be SPP1v1, while it was SPP1v2 in UC tissue (**Figure 3A-C**).

Identification of putative OPN targets

Next, we sought to identify putative OPN targets by analyzing the expression of previously described OPN receptors in various cell types. This analysis comprised the previously as a receptor for hyaluronic acids described glycoprotein CD44 including its alternative splicing variants (CD44, CD44 variant 3, CD44 variant 6, CD44 variant 7) and various integrin α and b chains that had previously been described to transmit OPN signals (**Figure 4**). Of note, the spatial resolution of the Xenium-RNA expression analysis allowed to take relative locational proximities of the respective gene expressions into consideration. This analysis revealed that CD44 is expressed in multiple cell types in CAC and there was little to no expression of CD44 splice variants. CD44 immunostainings revealed its expression on OPN+ macrophages, indicating an autocrine loop. Xenium RNA expression identified ITGαV and ITGβ6 in CAC epithelial clusters samples (**Figure 4A-E**). Further exploration of top DEG's in epithelial cluser revealed strong expression of Claudin 7. This tumour cluster showed strong expression of KRT7, EPCAM, CTNNB1 and GLUT1 **(Figure 5 A-B)**.

Immunosuppressive Niche in CAC

We identified a skew in the tissue distribution of lymphocytes within CACs: Regions with strong OPN expression were devoid of CD8^{+} T-lymphocytes and vice versa (i.e. regions with low OPN expression were CD8^{+} lymphocyte-rich (**Figure 6A-C**). Together with the fact, that the gene set analysis of the Nanostring RNA expression had pointed to a downregulation of (CD8^{+} lymphocyte signaling) and (lymphocyte activation) and that others had shown a function for OPN in CD8^{+} lymphocyte activation in experimental murine colitis (Klement, 2018), we hypothesized, that OPN might suppress CD8^{+} lymphocyte-related tumor surveillance processes in CAC.

Epithelial-to-mesenchymal transformation as a putative mechanism for OPN action on CACs

It has been previously described for OPN, that it activates epithelial-to-mesenchymal transition (EMT) as one pathway having the potential to contribute to carcinogenesis. In our data set and in line with this assumption, the transcription factor ZEB1 and the extracellular matrix protein fibronectin (FN1) were amongst the most up-regulated genes (**Tables 2 and 3**). To further substantiate these findings, immunostainings were performed for EpCAM, E-cadherin (**Figure 7A-B**) and vimentin (data not shown). Interestingly, blinded analysis of the slides revealed a tendency for lower EpCAM and lower E-cadherin but higher expression of vimentin in CAC tissues, supporting the hypothesis that EMT might be an active process in CAC (**Figure 7A**).

To clarify, if OPN might have the potential to induce EMT in the process of colitis-associated carcinogenesis, we established these organoids from healthy donors, UC patients (Sato 2011). and CAC patients (Fujii 2018, Driehuis 2020). These organoids expressed high levels of putative OPN

receptors including CD44 and Integrins when grown in stem cell medium. We then performed a series of RT-qPCR analyses to identify the effects of OPN, these gene panels included EMT genes, cell lineage genes and genes that were reported previously to be induced by OPN stimulus. However, these genes were not regulated by OPN stimulus and furthermore RNA sequencing analysis confirmed the following results (**Figure 8**) that these UC organoids do not respond to OPN, indicating an indirect role of OPN dependent tumorigenesis in CAC.

Materials and Methods

Nanostring Immunology v2 panel

We obtained FFPE specimens (Charité Biobank) from 40 patients that suffered from either one of the IBDs or CACs and furthermore inflammation-free healthy controls (10 patients per group). These samples were micro-dissected, followed by RNA isolation and Nanostring gene expression analysis using the Immunology v2 panel (630 genes).

Spatially resolved transcriptomics

To spatially resolve expression of a set of 477 genes at a sub-cellular resolution, we analyzed surgical FFPE tissue sections of UC and UC-CAC patients using the Xenium platform from 10x Genomics. We used the Human Multi-tissue and Cancer panel as base and added 100 custom genes, these genes were selected on the basis of SPP1 biology and tumour microenvironment.

Xenium sample preparation, imaging, and segmentation

Samples were processed according to manufacturer protocols "Xenium In Situ for FFPE – Tissue Preparation Guide CG000578 | Rev C", "Probe Hybridization, Ligation & Amplification, User Guide CG0000582" and "Decoding & Imaging, User Guide CG000584. Briefly, 5 μm thick sections were prepared from FFPE tissue of UCCAC(n=3), UC(n=3 and HC(n=1). All 3 UCCAC tissue sections were placed on one slide and all 3 UC and 1 HC tissues were placed on the second slide. This was followed by deparaffinization & decrosslinking of the sections. Slides were then placed in xenium cassettes and padlock probes were incubated overnight, followed by rolling circle amplification, autofluorescence quenching and nuclear staining. Slides were added to the Xenium Instrument for FOV selection followed by the iterative cyclic imaging. Segmentation data and transcript level decoding data was generated on board using xenium-1.6.0.8 analysis software.

Transcriptomic clustering of segmented cells

For downstream analysis, we used the package Seurat (v 5.0.1) (Stuart 2019) in R (v4.3.2). We followed the vignette from Satija Lab. (https://satijalab.org/seurat/articles/seurat5_spatial_vignette_2). Briefly, SCTransform was performed on all samples followed by filtering out cells with less than 20 genes. We then merged the CAC (n=3) gene matrices and UC (n=3) gene matrices into seurat objects. SCT was set as default assay followed by computing principal components (PCs) in 30 dimensions. We then selected these PC's and used FindNeighbour and RunUMAP functions. We then portioned the shared nearest neighbour (SNN) graph using a resolution of 0.5 and identified 28 clusters in UCCAC and 23 clusters in UC. To identify the DEG in each cluster, we used PrepSCTFindmarkers function.

DNA extraction

gDNA extraction from formalin-fixed paraffin-embedded (FFPE) tissue sections was carried out using Maxwell 16 FFPE plus LEV DNA purification kit (AS1720; Promega, Madison, WI, USA) according to the manufacturer's protocol. Subsequently, fluorescence-based quantification was performed using the Qubit dsDNA HS assay kit (Thermo Fisher Scientific, Waltham, MA, USA).

Cancer Hot Spot Panel-2 (CHP2) DNA sequencing and variant reporting

Mutations were detected by the automated Chef-ready Cancer Hotspot Panel v.2 according to the manufacturer's protocol (Thermo Fisher Scientific, Waltham, MA, USA). Briefly, optimally 50 ng DNA (lowest 10 ng) was used as input material and loaded on to the Ion Chef Instrument. After automated library preparation, the 100 pM library pool was diluted to 35 pM, amplified on Ion Sphere Particles with Ion 510&520&530 Kit-Chef and sequenced on the Ion S5 XL using Ion 530 Chips (Thermo Fisher Scientific, Waltham, MA, USA). Variants were identified using BAM files analyzed with JSI Sequence Pilot, SeqNext V5.4.0 (JSI Medical Systems GmbH, Kippenheim, Germany) and hg19 as human reference genome. Initial screening focused on detected variants with an allele frequency of minimum 5 %. Additionally, all variants with a allele frequency lower than 5 %, but a sequencing depth of 200x were revised and documented. The pathogenicity and knowledge status of those variants were checked in publicly available databases (cBioPortal, ClinVar, dbSNP) (Cerami E *et al.*, 2012; Gao J *et al.*, 2013; de Bruijn et al. 2023; Landrum et al. 2018; Sherry et al. 2001). Further interpretation focused on pathogenic, likely pathogenic or variants of unknown significance, synonymous, benign or likely benign mutations were not reported.

Organoid Culture

Human colon organoids were generated as described by Sato et. al. 2011 and Bartfeld et. al 2015. Briefly, colon endoscopy was performed using macro forceps and the biopsies were collected in ice cold basal medium containing Y(10uM). Biopsies were finely chopped, collected in a 50mL falcon tube and washed three times with 10mL of washed with ice cold PBS - (Gibco, Thermo Fisher Scientific Inc., Waltham, USA) until a clear supernatant was obtained and incubated in 2mM EDTA (Sigma) in PBS++ (Gibco, Thermo Fisher Scientific Inc., Waltham, USA) for 10 minutes at room temperature. After removal of EDTA, tissue fragments were washed with cold PBS. The fragments were then collected and added on a petridish and with the help of the glass slide, pressure was applied to release the crypts. Tissue fragments along with the released crypts were collected in 10mL ice cold basal medium and was mixed properly followed by incubation on ice for 5 min. Supernatant containing crypts was carefully collected and centrifuged at 500g for 5 min. The cell pellet was resuspended in Growth Factor Reduced Matrigel (Corning 354230) and cultured at 37 °C in the presence of 5% CO_2. The organoids were then overlaid medium containing 50% CM LWRN, 20% CM R spondin, 10% CM Noggin, Primocin, Y and recombinant human EGF and 10% cocktail of factors which includes B27,N2, Nac, Nic, SB202190, A83-01.

Table 1: Clinicopathological characteristics.

		Control	CD	UC	CDAC	UCAC
Gender f, m		5, 5	6, 4	3, 7	7, 3	5, 5
Age (range)		62 (52-80)	42 (20-61)	34,5 (19-51)	47 (31-90)	45,5 (36-78)
Inflammatory activity	High	-	5	6	3	3
	Low	-	5	4	1	7[4]
	None	10	-	-	6	
Location (inflammation/ tumor)	Pancolitis/ multilocular tumor	-	8[1]	7	-	2
	Right Hemicolon	-	-	-	5	1
	Transverse Colon	-	-	-	0	1
	Left Hemicolon	-	2	3	4	4
	Rectum	-	-	-	1	2
	Ileum	-	3	-	-	-
Duration of disease (range)		-	14,5 (4-27)	8 (0-24) 1 pat. N.a.	20 (3-37) 3 pat. n.a.	18 (1-39)
Tumor Type	Mucinous	-	-	-	6	9
	Non-mucinous	-	-	-	4	1
Tumor Stage (T)	pT1:	-	-	-	1	2
	pT2:	-	-	-	2	1
	pT3:	-	-	-	2	4
	pT4:	-	-	-	5	3
	N0:	-	-	-	6	4
	N1a:	-	-	-	2	3
	N2:	-	-	-	2	3
	M0:	-	-	-	8	8
	M1:	-	-	-	2[3]	2[7]
Recurrent Tumor(s)		-	-	-	0	0
Adenoma(s) present		1	0	1	2	6
Steroid treatment		-	7	8	2 (8 n.a.)	4 (4 n.a.)
Biological treatment		-	9	8	1 (7 n.a.)	0 (6 n.a.)

Age and duration of disease values correspond to the median in years.

[1], 1 of the above had segmental colitis sparing the transverse Colon

[2], 2 liver, 1 liver and peritoneum, 1 lung

[3], 1 liver, 1 peritoneum

[4], Histologically reported inflammation without activity level was counted as low/moderate for this synopsis

[6], 1 Patient: Unknown tumor spread

[7], 2 peritoneum

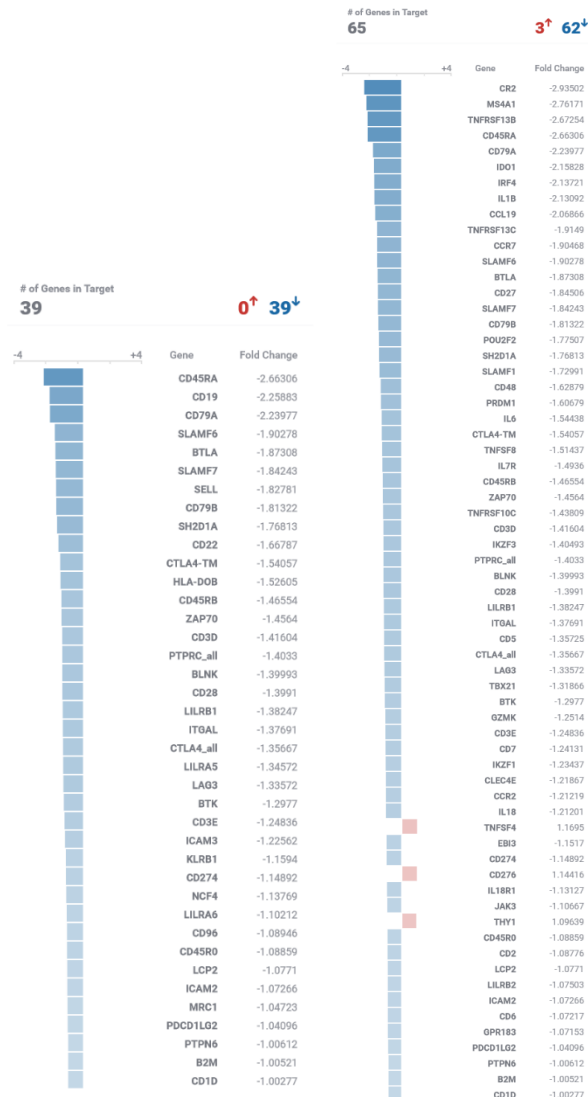**Table 2: 10 most up- and down-regulated genes in CDAC *vs.* CD.**

	Gene	Fold change	p-value
Up-regulated genes	SPP1	18,29	<0,001
	FN1	6,68	<0,001
	DUSP4	4,60	<0,001
	CLDN2	4,40	0,034
	CCL26	3,42	<0,001
	CD276	3,01	<0,001
	THY1	2,83	0,009
	ICAM5	2,78	0,010
	F2RL2	2,77	0,010
	CLEC5A	2,74	0,012
Down-regulated genes	PIGR	-23,69	<0,001
	CXCL13	-11,11	<0,001
	MS4A1	-9,77	<0,001
	CD79A	-7,51	<0,001
	NOS2	-7,34	0,002
	CR2	-6,58	<0,001
	CCL19	-6,44	<0,001
	PTPRC (RA)	-6,33	<0,001
	TNFRSF17	-6,12	<0,001
	TNFRSF13B	-5,38	<0,001

Table 3: 10 most up- and down-regulated genes in UCAC *vs.* UC

	Gene	Fold change	p-value
Up-regulated genes	SPP1	8,41	<0,001
	CCL26	2,91	0,022
	GRHL2	2,71	<0,001
	DUSP4	2,67	0,030
	CCND1	2,65	0,014
	FN1	2,22	0,039
	CEACAM6	2,05	0,032
	CD9	1,78	0,013
	SRC	1,70	0,011
	TRAF2	1,68	0,008
Down-regulated genes	DEFB4A	-18,33	<0,001
	S100A8	-14,97	<0,001
	PIGR	-11,10	0,011
	NOS2	-10,15	<0,001
	S100A9	-8,56	<0,001
	MS4A1	-8,20	<0,001
	IRF4	-7,90	<0,001
	CXCL13	-7,31	0,001
	TNFRSF13B	-7,26	0,001
	IL1B	-7,00	<0,001

Table 4: Analysis of gene sets

	No of genes included	Up- (↑) / down- (↓) regulated genes	Directed significance score
MHC II antigen presentation	14	5↓	-3.18
Adaptive immune system	137	39↓	-3.12
Lymphocyte activation	241	3↑ 62↓	-3.07
TNF family signaling	49	7↓	-2.74
Cell adhesion	56	2↑ 17↓	-2.57
Cytokine signaling	259	3↑ 44↓	-2.55
NF-κB signaling	62	10↓	-2.53

# of Genes in Target: 39   0↑ 39↓

Gene	Fold Change
CD45RA	-2.66306
CD19	-2.25883
CD79A	-2.23977
SLAMF6	-1.90278
BTLA	-1.87308
SLAMF7	-1.84243
SELL	-1.82781
CD79B	-1.81322
SH2D1A	-1.76813
CD22	-1.66787
CTLA4-TM	-1.54057
HLA-DOB	-1.52605
CD45RB	-1.46554
ZAP70	-1.4564
CD3D	-1.41604
PTPRC_all	-1.4033
BLNK	-1.39993
CD28	-1.3991
LILRB1	-1.38247
ITGAL	-1.37691
CTLA4_all	-1.35667
LILRA5	-1.34572
LAG3	-1.33572
BTK	-1.2977
CD3E	-1.24836
ICAM3	-1.22562
KLRB1	-1.1594
CD274	-1.14892
NCF4	-1.13769
LILRA6	-1.10212
CD96	-1.08946
CD45R0	-1.08859
LCP2	-1.0771
ICAM2	-1.07266
MRC1	-1.04723
PDCD1LG2	-1.04096
PTPN6	-1.00612
B2M	-1.00521
CD1D	-1.00277

# of Genes in Target: 65   3↑ 62↓

Gene	Fold Change
CR2	-2.93502
MS4A1	-2.76171
TNFRSF13B	-2.67254
CD45RA	-2.66306
CD79A	-2.23977
IDO1	-2.15828
IRF4	-2.13721
IL1B	-2.13092
CCL19	-2.06866
TNFRSF13C	-1.9149
CCR7	-1.90468
SLAMF6	-1.90278
BTLA	-1.87308
CD27	-1.84506
SLAMF7	-1.84243
CD79B	-1.81322
POU2F2	-1.77507
SH2D1A	-1.76813
SLAMF1	-1.72991
CD48	-1.62879
PRDM1	-1.60679
IL6	-1.54438
CTLA4-TM	-1.54057
TNFSF8	-1.51437
IL7R	-1.4936
CD45RB	-1.46554
ZAP70	-1.4564
TNFRSF10C	-1.43809
CD3D	-1.41604
IKZF3	-1.40493
PTPRC_all	-1.4033
BLNK	-1.39993
CD28	-1.3991
LILRB1	-1.38247
ITGAL	-1.37691
CD5	-1.35725
CTLA4_all	-1.35667
LAG3	-1.33572
TBX21	-1.31866
BTK	-1.2977
GZMK	-1.2514
CD3E	-1.24836
CD7	-1.24131
IKZF1	-1.23437
CLEC4E	-1.21867
CCR2	-1.21219
IL18	-1.21201
TNFSF4	1.1695
EBI3	-1.1517
CD274	-1.14892
CD276	1.14416
IL18R1	-1.13127
JAK3	-1.10667
THY1	1.09639
CD45R0	-1.08859
CD2	-1.08776
LCP2	-1.0771
LILRB2	-1.07503
ICAM2	-1.07266
CD6	-1.07217
GPR183	-1.07153
PDCD1LG2	-1.04096
PTPN6	-1.00612
B2M	-1.00521
CD1D	-1.00277

Adaptive Immune System
Bar to the left
pink: downregulated genes

Chemokine Signaling

green: upregulated genes
pink: downregulated genes

References

1. Beaugerie L, Itzkowitz SH. Cancers complicating inflammatory bowel disease. N Engl J Med 2015;372:1441-52.
2. Foersch S, Neurath MF. Colitis-associated neoplasia: molecular basis and clinical translation. Cell Mol Life Sci 2014;71:3523-35.
3. Herszenyi L, Barabas L, Miheller P, et al. Colorectal cancer in patients with inflammatory bowel disease: the true impact of the risk. Dig Dis 2015;33:52-7.
4. Rutter MD, Saunders BP, Wilkinson KH, et al. Thirty-year analysis of a colonoscopic surveillance program for neoplasia in ulcerative colitis. Gastroenterology 2006;130:1030-8.
5. Jess T, Rungoe C, Peyrin-Biroulet L. Risk of colorectal cancer in patients with ulcerative colitis: a meta-analysis of population-based cohort studies. Clin Gastroenterol Hepatol 2012;10:639-45.
6. Grivennikov SI. Inflammation and colorectal cancer: colitis-associated neoplasia. Semin Immunopathol 2013;35:229-44.
7. Yaeger R, Shah MA, Miller VA, et al. Genomic Alterations Observed in Colitis-Associated Cancers Are Distinct From Those Found in Sporadic Colorectal Cancers and Vary by Type of Inflammatory Bowel Disease. Gastroenterology 2016;151:278-287 e6.
8. Cooks T, Pateras IS, Tarcic O, et al. Mutant p53 prolongs NF-kappaB activation and promotes chronic inflammation and inflammation-associated colorectal cancer. Cancer Cell 2013;23:634-46.
9. Becker C, Fantini MC, Schramm C, et al. TGF-beta suppresses tumor progression in colon cancer by inhibition of IL-6 trans-signaling. Immunity 2004;21:491-501.
10. Putoczki TL, Thiem S, Loving A, et al. Interleukin-11 is the dominant IL-6 family cytokine during gastrointestinal tumorigenesis and can be targeted therapeutically. Cancer Cell 2013;24:257-71.
11. Popivanova BK, Kitamura K, Wu Y, et al. Blocking TNF-alpha in mice reduces colorectal carcinogenesis associated with chronic colitis. J Clin Invest 2008;118:560-70.
12. Durant L, Watford WT, Ramos HL, et al. Diverse targets of the transcription factor STAT3 contribute to T cell pathogenicity and homeostasis. Immunity 2010;32:605-15.
13. Huber S, Gagliani N, Zenewicz LA, et al. IL-22BP is regulated by the inflammasome and modulates tumorigenesis in the intestine. Nature 2012;491:259-63.
14. Delbue D, Lebenheim, L., Cardoso-Silva, D. Reprogramming intestinal epithelial cell polarity by interleukin-22. Frontiers in Medicine 2021;in print.
15. Mani SA, Guo W, Liao MJ, et al. The epithelial-mesenchymal transition generates cells with properties of stem cells. Cell 2008;133:704-15.
16. Nanki K, Fujii M, Shimokawa M, et al. Somatic inflammatory gene mutations in human ulcerative colitis epithelium. Nature 2020;577:254-259.
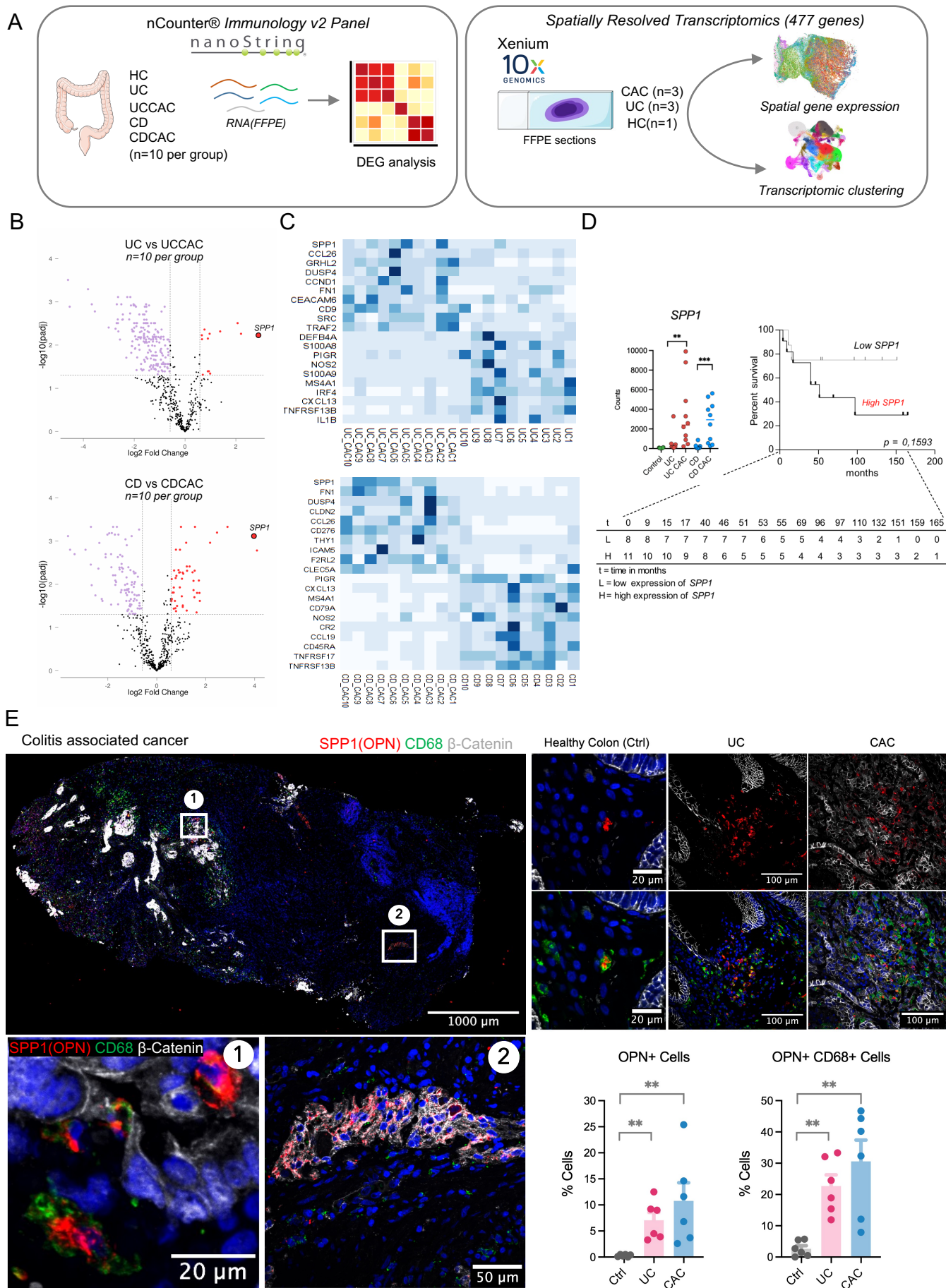
Figure 1

Figure 1. A. Study design. B Nanostring Immune Panel v2 Volcano plots of UC vs UCCAC and CD v CDCAC reveals SPP1 to be upregulated in both cohorts. C, Heatmaps with top 20 genes, D. KM plot using SPP1, E. Heterogenous OPN expression in CAC, F. Quantification of OPN expression across Control, UC and CAC patients (n=3).
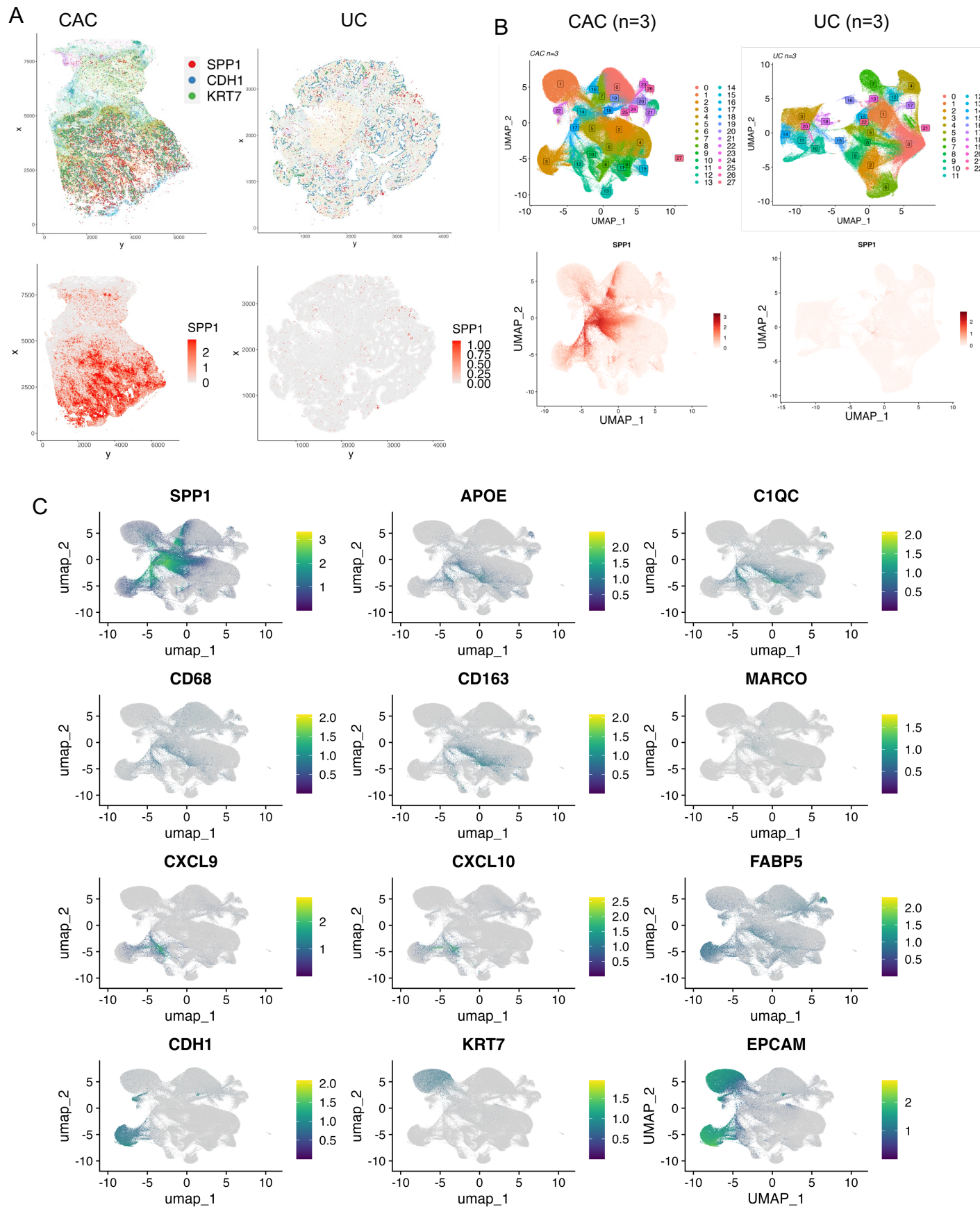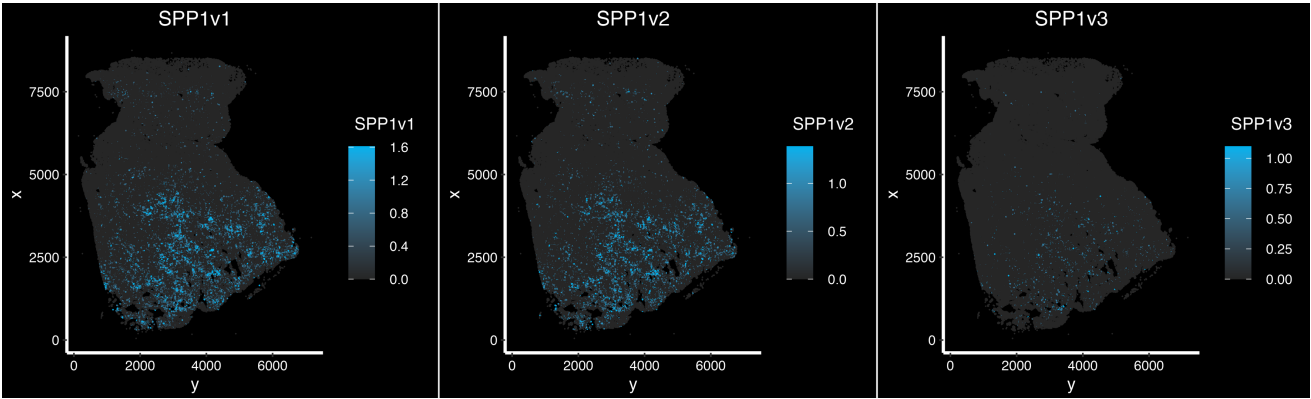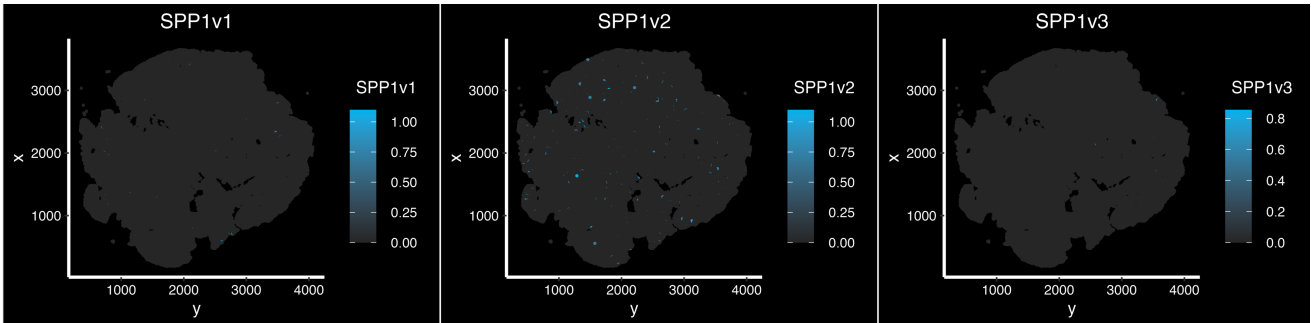
Figure 2

Figure2. Spatial heterogeneity of SPP1 expression in CAC. (A) Spatial gene expression plots of SPP1, CDH1 and KRT7 expression in CAC and UC (B) Unsupervised clustering results of CAC(n=3) and UC(n=3). (C) UMAP plots of genes in SPP1 macrophage cluster.

Figure 3

A CAC

B UC

C
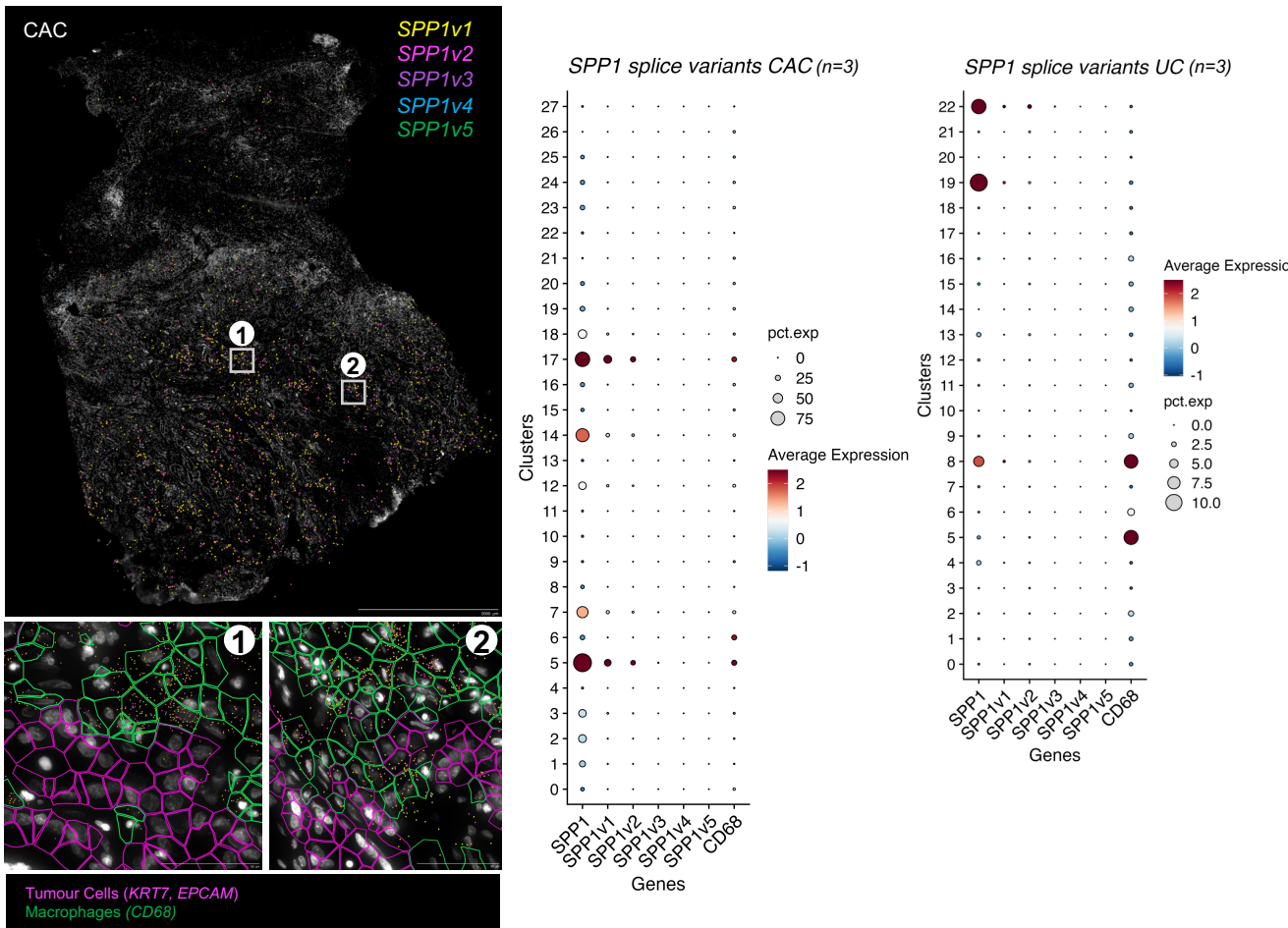
Figure 3. SPP1 splice variants in CAC and UC. A. SPP1v1, v2, v3 transcript density plots of CAC tissues, B. SPP1v1, v2, v3 transcript density plots of UC tissues, C. SPP1v1, v2, v3 transcript at single cell resolution in CAC, Dotplots showing the transcriptomic clusters and SPP1 splice variants in CAC and UC (n=3).

Figure 4

Figure 4. OPN Receptors in CAC. A, D, E. Density maps of CD44, Integrin aV and β6 expression in CAC B. CD44, Integrin aV and β6 transcripts at single cell resolution. F. Dotplots showing transcriptomic clusters in CAC and UMAPs of putative OPN receptors in UC and CAC (n=3).
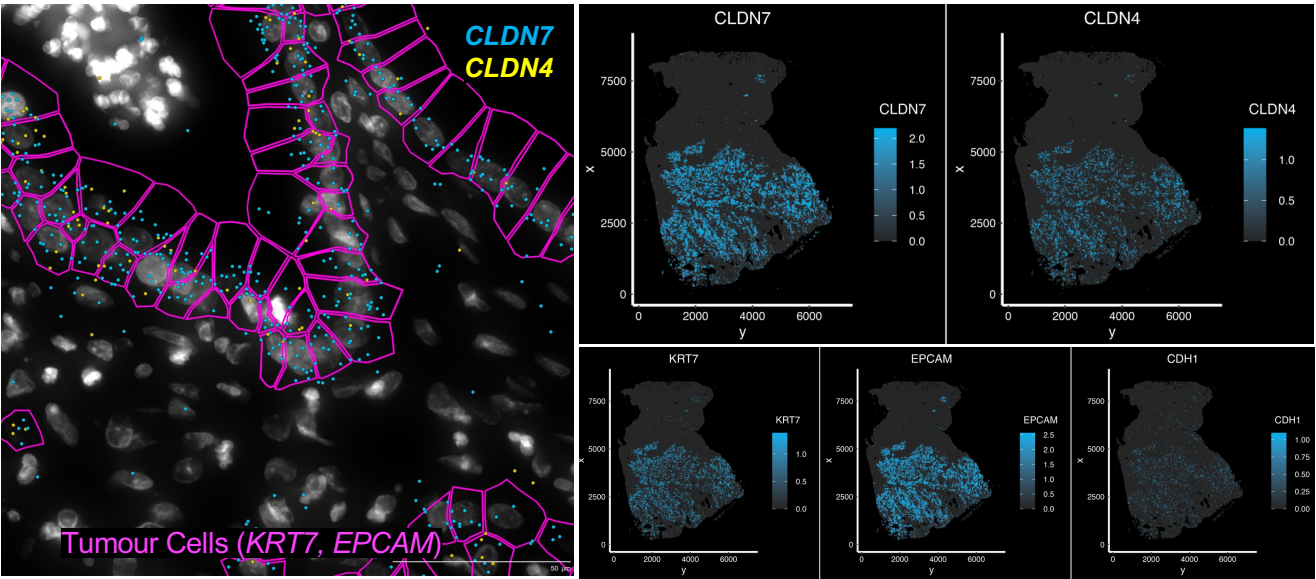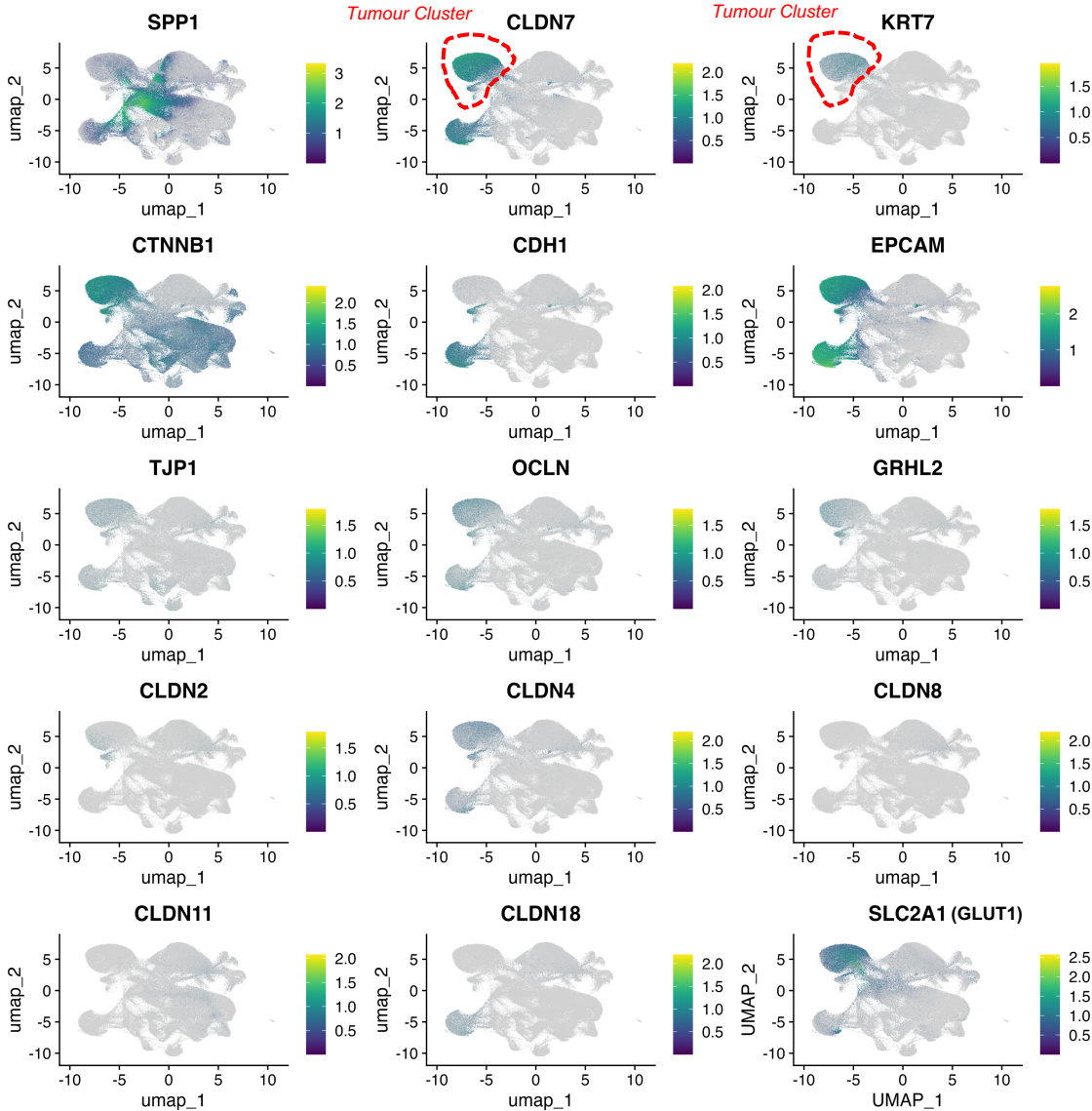
Figure 5

Figure 5. A. Tight Junction genes CLDN7 and CLDN 4 at a single cell resolution in CAC. B. UMAPs of TJ genes in CAC.
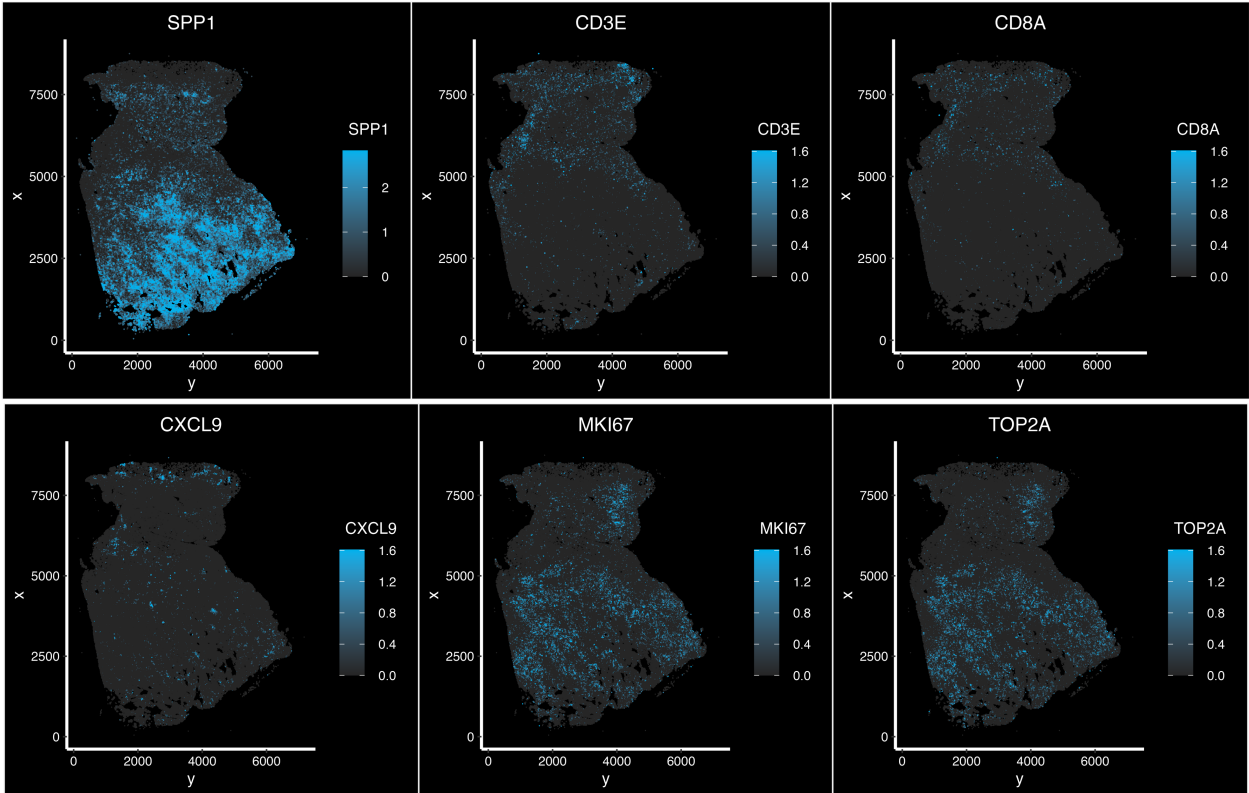
Figure 6

A
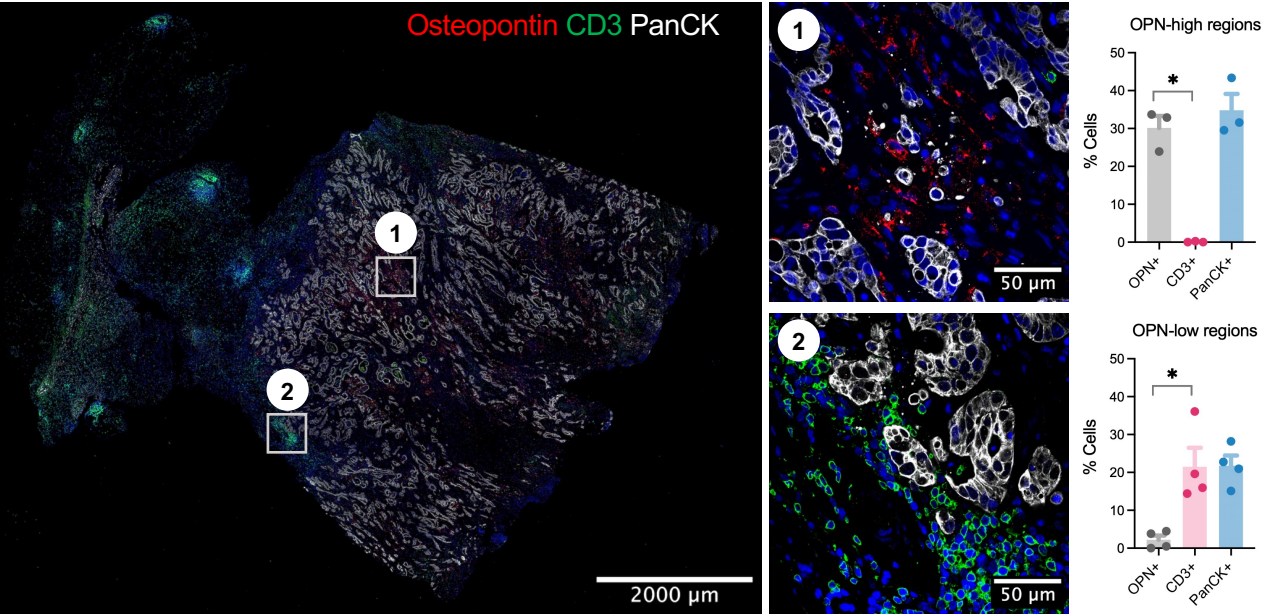
B
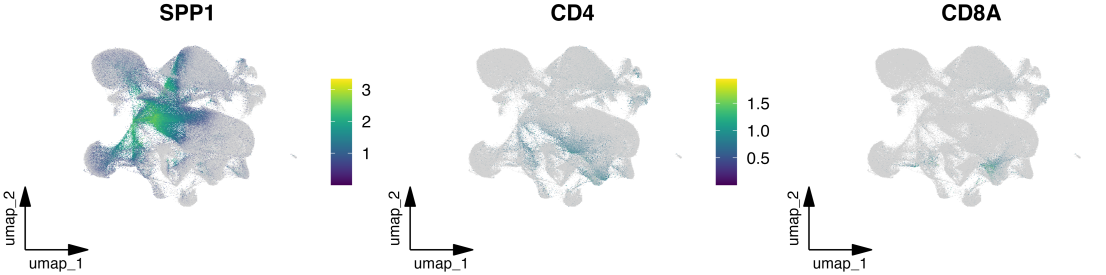
C

Figure 6. Immunosuppressive niche in CAC. A. Immunostainings of CAC tissues showing mutually exclusive expression of OPN and CD3. B. UMAP plots of CAC showing SPP1, CD4 and CD8A clusters. C. Transcript density maps of SPP1, CXCL9, CD3, CD8A and cell cycle genes.
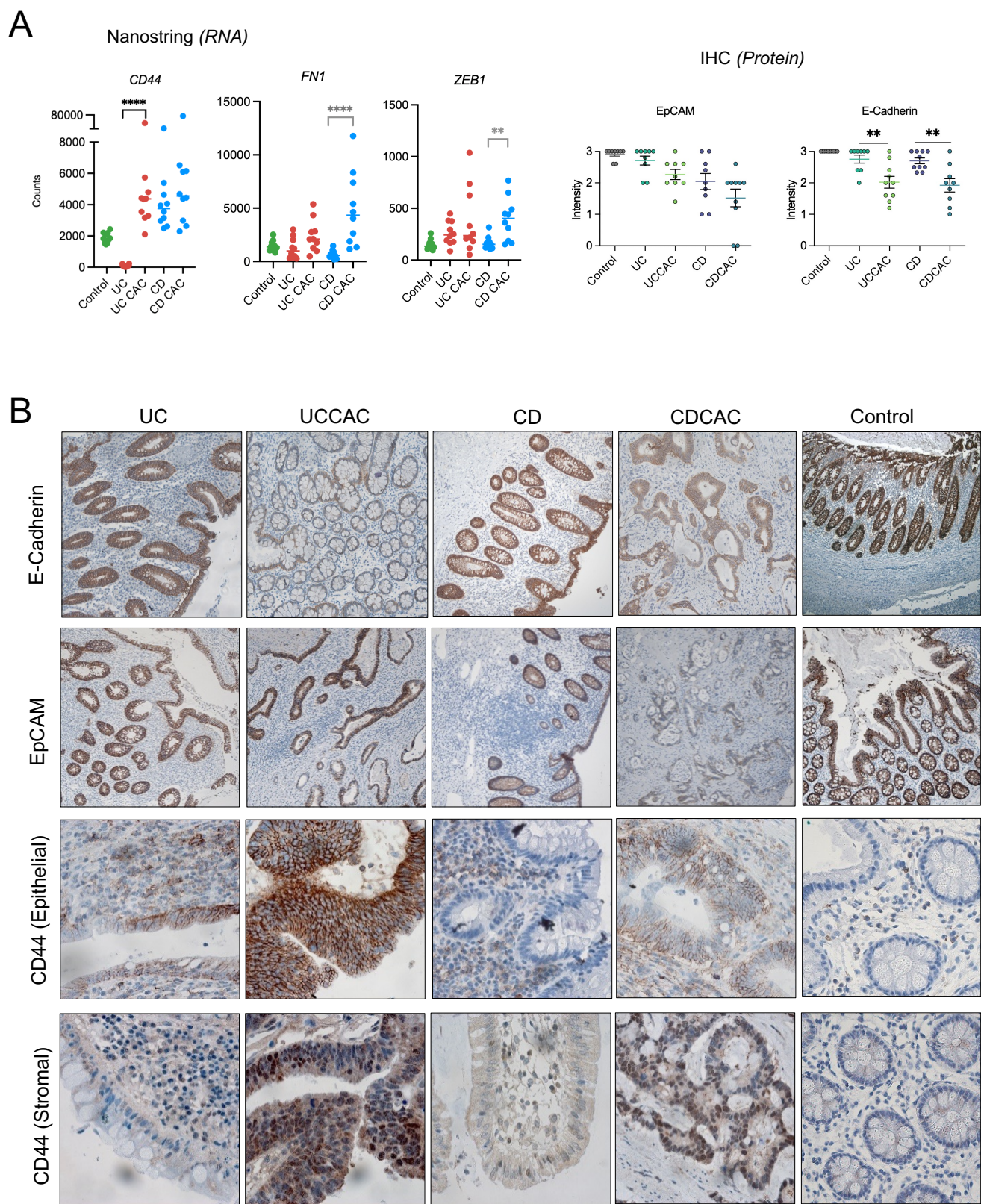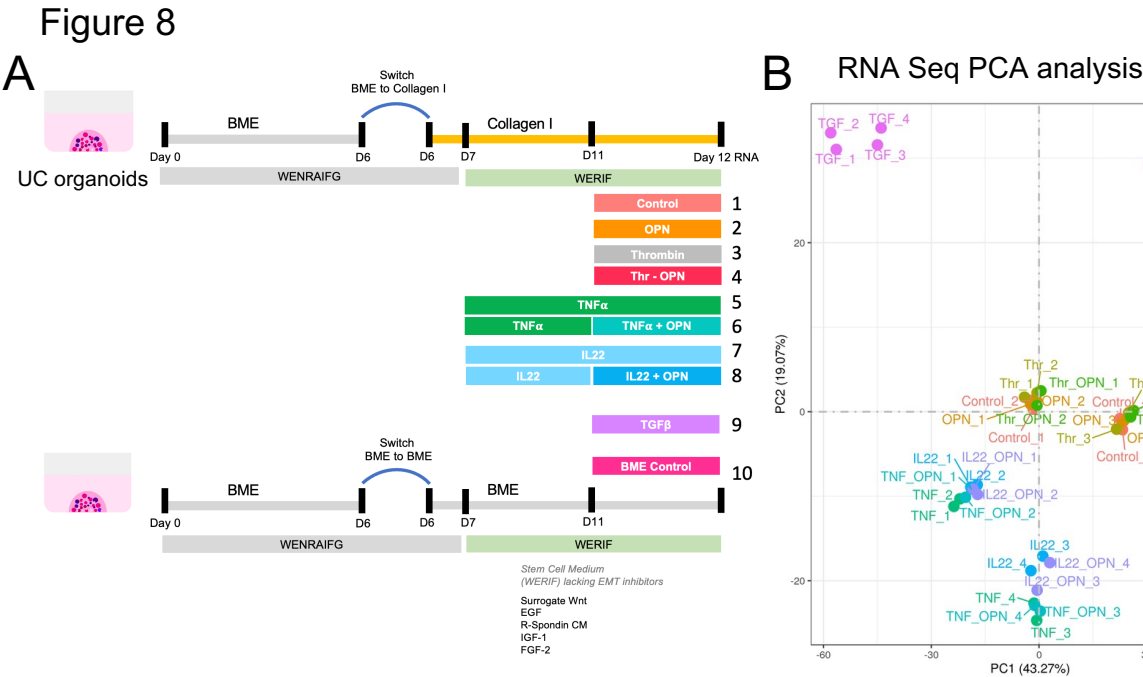
Figure 7

A

Nanostring *(RNA)*

IHC *(Protein)*

B

Figure 7. EMT in CAC. A. Nanostring gene expression dotplots showing EMT genes CD44, FN1 and ZEB1. B. IHC staining of epithelial proteins E-Cadherin, EpCAM and CD44 in UC, UCCAC, CD, CDCAC and Controls(n=10 per group)

Figure 8

A

B
RNA Seq PCA analysis

C

| Comparison	Total DEG	Up Genes	Down Genes	Method
Control vs OPN	0	0	0	DESeq2 padj <=0.05, log2FC>1.5
Thr vs Thr_OPN	0	0	0	DESeq2 padj <=0.05, log2FC>1.5
TNFα vs TNFα_OPN	0	0	0	DESeq2 padj <=0.05, log2FC>1.5
IL22 vs IL22_OPN	0	0	0	DESeq2 padj <=0.05, log2FC>1.5
Control vs TGFβ	3329	1773	1558	DESeq2 padj <=0.05, log2FC>1.5
Control vs IL22	502	267	235	DESeq2 padj <=0.05, log2FC>1.5
Matrigel vs Collagen	1814	487	1327	DESeq2 padj <=0.05, log2FC>1.5

D
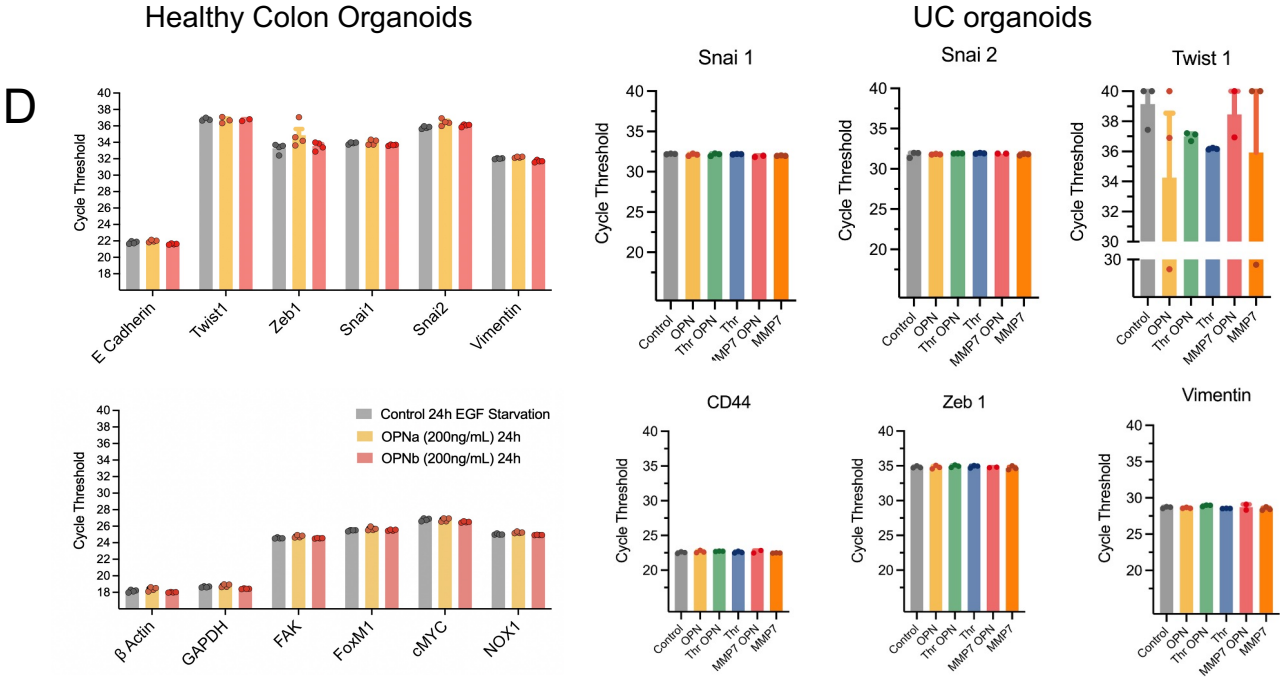
Figure 8. RNA Seq analysis of UC organoids. A. Experimental details of OPN stimulated UC organoids. B. PCA analysis of OPN stimulated UC organoids. C. Table of differentially expressed genes in UC organoids in response to OPN. D. RT-qPCR analysis EMT genes in colon organoid stimulated with OPN.

Supplementary Figure 1
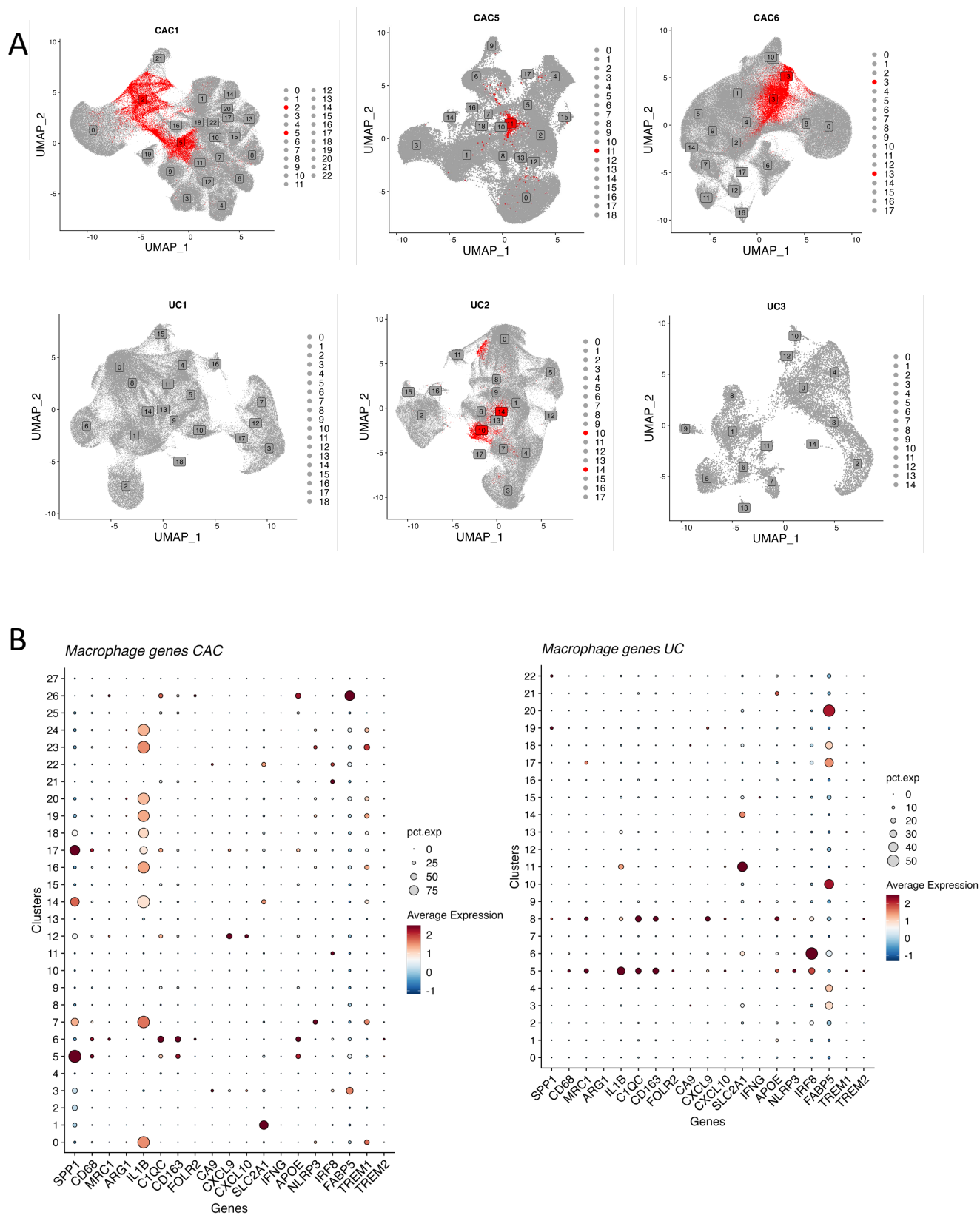
Supplementary Figure 1. *SPP1*⁺ macrophage clusters are present uniformly across CAC patients. B. *SPP1*⁺ macrophage subset in CAC